

A Refined Space Vector PWM Signal Generation for Seven-Level Inverter

G.Sambasiva Rao¹ K.Chandra Sekhar²

Abstract– A refined space vector modulation scheme for a seven-level inverter system for dual-fed induction motor drive, using only the instantaneous sampled reference signals is presented in this paper. The dual-fed structure is realized by opening the neutral-point of the conventional squirrel cage induction motor. The seven-level inversion is obtained by feeding the dual-fed induction motor with two symmetrical three-level inverters from both ends. The proposed space vector pulse width modulation technique does not require the sector information and look-up tables to select the appropriate switching vectors. The inverter leg switching times are directly obtained from the instantaneous sampled reference signal amplitudes and centers the switching times for the middle space vectors in a sampling time interval, as in the case of conventional space vector pulse width modulation.

Keywords– dual-fed induction motor, seven-level inverter, space vector PWM, sampled sinusoidal reference signals, middle space vectors.

I. INTRODUCTION

The two most widely used pulse width modulation (PWM) schemes for multilevel inverters are the carrier-based sine-triangle PWM (SPWM) scheme and the space vector PWM (SVPWM) scheme. These modulation schemes have been extensively studied and compared for the performance parameters with two level inverters [1],[2]. The SPWM schemes are more flexible and simpler to implement, but the maximum peak of the fundamental component in the output voltage is limited to 50% of the DC link voltage [2]. In SVPWM schemes, a reference space vector is sampled at regular intervals to determine the inverter switching vectors and their time durations, in a sampling time interval. The SVPWM scheme gives a more fundamental voltage and better harmonic performance compared to the SPWM schemes [3-5]. The maximum peak of the fundamental component in the output voltage obtained with SVPWM is 15% greater than with the SPWM scheme [2],[3]. But the conventional SVPWM scheme requires sector identification and look-up tables to determine the timings for various switching vectors of the inverter, in all the sectors [3],[4]. This makes the implementation of the SVPWM scheme quite complicated. It has been shown that, for two-level inverters, a SVPWM like performance can be obtained with a SPWM scheme by adding a common mode voltage of suitable magnitude, to the sinusoidal reference signals [4],[5]. A simplified method, to determine the correct offset times for centering

the time durations of the middle space vectors, in a sampling time interval, is presented [8], for the two-level inverter. The inverter leg switching times are calculated directly from the sampled amplitudes of the sinusoidal reference signals with considerable reduction in the computation time [8].

The SPWM scheme, when applied to multilevel inverters, uses a number of level-shifted carrier signals to compare with the sinusoidal reference signals [9]. The SVPWM for multilevel inverters [10],[11] involves mapping of the outer sectors to an inner subhexagon sector, to determine the switching time interval, for various space vectors. Then the switching space vectors corresponding to the actual sector are switched, for the time durations calculated from the mapped inner sectors. It is obvious that such a scheme, in multilevel inverters, will be very complex, as a large number of sectors and inverter vectors are involved. This will also considerably increase the computation time.

A modulation scheme is presented in [12], where a fixed common mode voltage is added to the reference signal throughout the modulation range. It has been shown [13] that this common mode addition will not result in a SVPWM-like performance, as it will not centre the middle space vectors in a sampling interval. The common mode voltage to be added in the reference phase voltages, to achieve SVPWM-like performance, is a function of the modulation index for multilevel inverters [13]. A SVPWM scheme based on the above principle has been presented [14], where the switching time for the inverter legs is directly determined from sampled sinusoidal reference signal amplitudes. This technique reduces the computation time considerably more than the conventional SVPWM techniques do, but it involves region identifications based on modulation indices. While this SVPWM scheme works well for a three-level PWM generation, it cannot be extended to multilevel inverters of levels higher than three, as the region identification becomes more complicated. A carrier-based PWM scheme has been presented [15], where sinusoidal references are added with a proper offset voltage before being compared with carriers, to achieve the performance of a SVPWM. The offset voltage computation is based on a modulus function depending on the DC link voltage, number of levels and the sinusoidal reference signal amplitudes. A SVPWM scheme is presented [18], where the switching time for the inverter legs is directly determined from sampled sinusoidal reference signal amplitudes for five-level inverter. A carrier based SPWM scheme is presented [19],[20], for five-level and seven-level inverter.

The objective of this paper is to present an implementation scheme for PWM signal generation for seven-level inverter system for dual-fed induction motor, similar to the

The paper first received 2 June 2011 and in revised form 2 May 2012.

Digital Ref: A190711112

¹ Department of Electrical Engineering, R.V.R and J.C College of Engineering, Chowdavaram, Guntur -522 019(India)

E-mail: sambasiva.gudapati@gmail.com

² Professor, Department of Electrical Engineering, R.V.R and J.C College of Engineering, Chowdavaram, Guntur -522 019(India)

E-mail: cskoritala@gmail.com

SVPWM scheme. In the proposed scheme, the dual-fed induction motor is fed with two symmetrical three-level inverters from both ends. The PWM switching times for the inverter legs are directly derived from the sampled amplitudes of the sinusoidal reference signals. A simple way of adding an offset voltage to the sinusoidal reference signals, to generate the SVPWM pattern, from only the sampled amplitudes of sinusoidal reference signals, is explained. The proposed SVPWM signal generation does not involve checks for region identification, as in the SVPWM scheme presented in [14]. Also, the algorithm does not require either sector identification or look-up tables for switching vector determination as are required in the conventional multilevel SVPWM schemes [10],[11]. Thus the scheme is computationally efficient when compared to conventional multilevel SVPWM schemes, making it superior for real-time implementation.

II. SEVEN-LEVEL INVERTER SCHEME FOR THE DUAL-FED INDUCTION MOTOR

The power circuit of the proposed drive is shown in Fig. 1. Two symmetrical three-level inverters, Inverter-A and Inverter-B feed the dual-fed induction motor. The inverter-A is composed of two conventional two-level inverters INV-1 and INV-2 in cascade. The Inverter-B is composed of two conventional two-level inverters INV-3 and INV-4 in cascade. The DC link voltages of INV-1, INV-2, INV-3 and INV-4 are $(2/6)E_{dc}$, $(2/6)E_{dc}$, $(1/6)E_{dc}$ and $(1/6)E_{dc}$ respectively, where E_{dc} is the DC link voltage of an equivalent conventional single two-level inverter drive.

The leg voltage E_{A2n} of phase-A attains a voltage of $(2/6)E_{dc}$ if the switches S_{21} and S_{14} are turned on. The leg voltage E_{A2n} of phase-A attains a voltage of $(4/6)E_{dc}$ if the switches S_{21} and S_{11} are turned on. The leg voltage E_{A2n} of phase-A attains a voltage of zero volts if the switch S_{24} is turned on. Thus the leg voltage E_{A2n} attains three voltages of 0, $(2/6)E_{dc}$ and $(4/6)E_{dc}$, which is basic characteristic of a 3-level inverter.

The leg voltage $E_{A4n'}$ of phase-A attains a voltage of $(1/6)E_{dc}$ if the switches S_{41} and S_{34} are turned on. The leg voltage $E_{A4n'}$ of phase-A attains a voltage of $(2/6)E_{dc}$ if the switches S_{41} and S_{31} are turned on. The leg voltage $E_{A4n'}$ of phase-A attains a voltage of zero volts if the switch S_{44} is turned on. Thus the leg voltage $E_{A4n'}$ attains three voltages of 0, $(1/6)E_{dc}$ and $(2/6)E_{dc}$, which is basic characteristic of a 3-level inverter.

Thus, one end of dual-fed induction motor may be connected to a DC link voltage of either zero or $(2/6)E_{dc}$ or $(4/6)E_{dc}$ and other end may be connected to a DC link voltage of either zero or $(1/6)E_{dc}$ or $(2/6)E_{dc}$. When both the inverters Inverter-A and Inverter-B drive the induction motor from both ends, seven different levels are attained by each phase of the induction motor. If we assume that the points n and n' are connected, the seven levels generated for phase-A are shown in Table1.

III. VOLTAGE SPACE VECTORS OF PROPOSED INVERTER

At any instant, the combined effect of 120° phase shifted three voltages in the three windings of the induction motor

Table1: The seven levels realized in the phase-A winding

Leg-voltage of phase A (E_{A2n})	Leg-voltage of phase A ($E_{A4n'}$)	Motor phase voltage $E_{A2A4} = E_{A2n} - E_{A4n'}$	Level
0	$(2/6)E_{dc}$	$-(2/6)E_{dc}$	Level 1
0	$(1/6)E_{dc}$	$-(1/6)E_{dc}$	Level 2
0	0	0	Level 3
$(2/6)E_{dc}$	$(1/6)E_{dc}$	$(1/6)E_{dc}$	Level 4
$(2/6)E_{dc}$	0	$(2/6)E_{dc}$	Level 5
$(4/6)E_{dc}$	$(1/6)E_{dc}$	$(3/6)E_{dc}$	Level 6
$(4/6)E_{dc}$	0	$(4/6)E_{dc}$	Level 7

could be represented by an equivalent space vector. This space vector E_s , for the proposed scheme is given by

$$E_s = E_{A2A4} + E_{B2B4}.e^{j(2\pi/3)} + E_{C2C4}.e^{j(4\pi/3)} \quad (1)$$

By substituting expressions for the equivalent phase voltages in (1),

$$E_s = (E_{A2n} - E_{A4n'}) + (E_{B2n} - E_{B4n'})e^{j(2\pi/3)} + (E_{C2n} - E_{C4n'})e^{j(4\pi/3)} \quad (2)$$

This equivalent space vector E_s can be determined by resolving the three phase voltages along mutually perpendicular axes, d-q axes of which d-axis is along the A-phase (Fig. 2). Then the space vector is given by

$$E_s = E_s(d) + jE_s(q) \quad (3)$$

Where $E_s(d)$ is the sum of all voltage components of E_{A2A4} , E_{B2B4} and E_{C2C4} along the d-axis and $E_s(q)$ is the sum of the voltage components of E_{A2A4} , E_{B2B4} and E_{C2C4} along the q-axis. The voltage components $E_s(d)$ and $E_s(q)$ can be thus expressed by the following transformation,

$$E_s(d) = E_{A2A4}(d) + E_{B2B4}(d) + E_{C2C4}(d) \quad (4)$$

$$E_s(q) = E_{B2B4}(q) + E_{C2C4}(q) \quad (5)$$

$$\begin{bmatrix} E_s(d) \\ E_s(q) \end{bmatrix} = \begin{bmatrix} 1 & -\frac{1}{2} & -\frac{1}{2} \\ 0 & \frac{\sqrt{3}}{2} & -\frac{\sqrt{3}}{2} \end{bmatrix} \begin{bmatrix} E_{A2A4} \\ E_{B2B4} \\ E_{C2C4} \end{bmatrix} \quad (6)$$

By substituting expressions for the equivalent phase voltages in (6),

$$\begin{bmatrix} E_s(d) \\ E_s(q) \end{bmatrix} = \begin{bmatrix} 1 & -\frac{1}{2} & -\frac{1}{2} \\ 0 & \frac{\sqrt{3}}{2} & -\frac{\sqrt{3}}{2} \end{bmatrix} \begin{bmatrix} E_{A2n} - E_{A4n'} \\ E_{B2n} - E_{B4n'} \\ E_{C2n} - E_{C4n'} \end{bmatrix} \quad (7)$$

The inverters can generate different levels of voltage vectors in the three phases of induction motor depending upon the condition of the switchings of inverter and for each of the different combinations of leg voltages, E_{A2n} , E_{B2n} and E_{C2n} for the inverter-A and $E_{A4n'}$, $E_{B4n'}$ and $E_{C4n'}$ for the inverter-B. The different equivalent voltage space vectors can be determined using (3) and (7). The possible combinations of space vectors will occupy different locations as shown in Fig. 3. There are in total 127 locations forming 216 sectors in the space vector point of view. The resultant hexagon (Fig. 3) can be divided into six layers: layer-1(innermost layer); layer-2(next outer layer); layer-3(layer outside layer-2); layer-4 (layer outside layer-3); layer-5 (layer outside layer-4) and layer-6 (outermost layer).

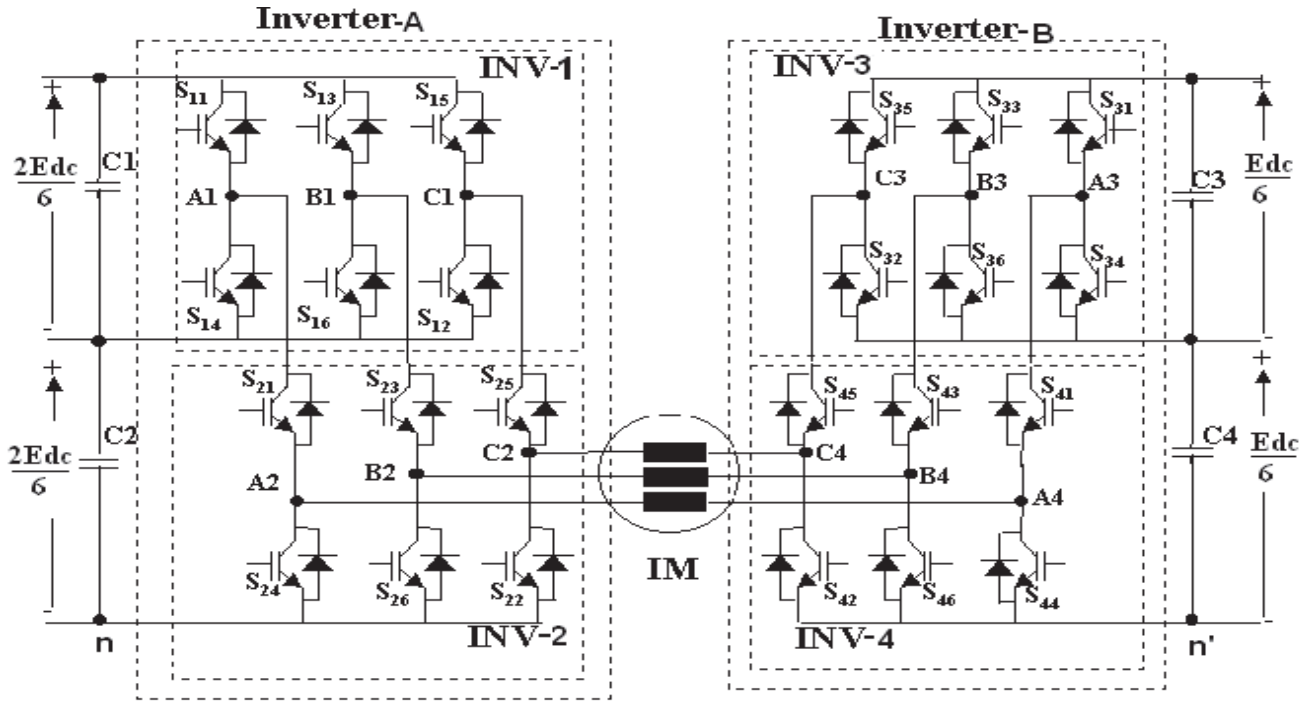


Fig. 1: Schematic circuit diagram of the proposed 7-level inverter drive scheme.

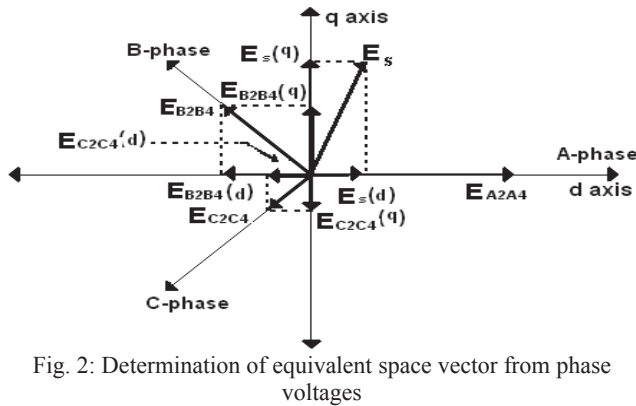


Fig. 2: Determination of equivalent space vector from phase voltages

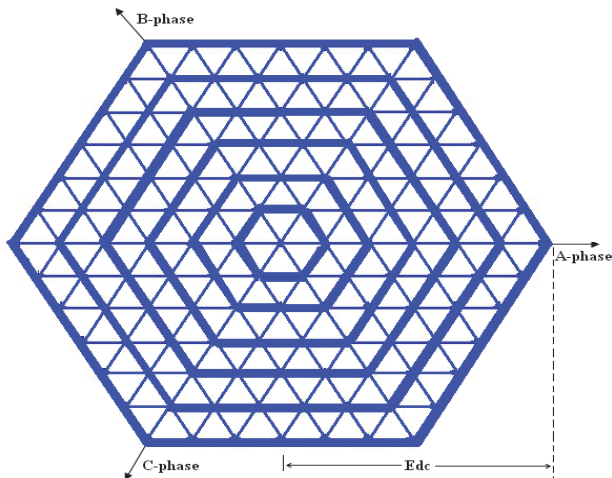


Fig. 3: The voltage space vector locations and layers for the proposed drive

IV. EFFECT OF COMMON-MODE VOLTAGE IN SPACE VECTOR LOCATIONS

In the above analysis to generate the different levels and the space vector locations, the points n and n' are assumed to be connected. When the points n and n' are not connected (as in the proposed topology, Fig. 1), the actual motor phase voltages are

$$E_{A2A4} = E_{A2n} - E_{A4n'} - E_{n'n} \quad (8)$$

$$E_{B2B4} = E_{B2n} - E_{B4n'} - E_{n'n} \quad (9)$$

$$E_{C2C4} = E_{C2n} - E_{C4n'} - E_{n'n} \quad (10)$$

$E_{n'n}$ is the common-mode voltage and is given by

$$E_{n'n} = \frac{1}{3}(E_{A2n} + E_{B2n} + E_{C2n}) - \frac{1}{3}(E_{A4n'} + E_{B4n'} + E_{C4n'}) \quad (11)$$

Substituting these expressions in (1)

$$\begin{aligned} E_s &= (E_{A2n} - E_{A4n'} - E_{n'n}) + (E_{B2n} - E_{B4n'} - E_{n'n})e^{j(2\pi/3)} \\ &\quad + (E_{C2n} - E_{C4n'} - E_{n'n})e^{j(4\pi/3)} = (E_{A2n} - E_{A4n'}) \\ &\quad + (E_{B2n} - E_{B4n'})e^{j(2\pi/3)} + (E_{C2n} - E_{C4n'})e^{j(4\pi/3)} \\ &\quad - (E_{n'n} + E_{n'n}e^{j(2\pi/3)} + E_{n'n}e^{j(4\pi/3)}) \end{aligned}$$

In this equation

$$(E_{n'n} + E_{n'n}e^{j(2\pi/3)} + E_{n'n}e^{j(4\pi/3)}) =$$

$$E_{n'n} - \frac{1}{2}E_{n'n} - \frac{1}{2}E_{n'n} = 0$$

and the equation then reduces to

$$\begin{aligned} E_s &= (E_{A2n} - E_{A4n'}) + (E_{B2n} - E_{B4n'})e^{j(2\pi/3)} \\ &\quad + (E_{C2n} - E_{C4n'})e^{j(4\pi/3)} \end{aligned}$$

This expression of E_s is the same as (2), where the points n and n' are assumed to be connected. The above analysis depicts that the common-mode voltage present between the points n and n' does not effect the space vector locations. This common-mode voltage will effect only in the diversity of space vectors in different locations.

V. PROPOSED SVPWM IN LINEAR MODULATION RANGE

For two-level inverters, in the SPWM scheme, each sinusoidal reference signal is compared with the triangular carrier signal and the individual phase voltages are generated [1]. To attain the maximum possible peak amplitude of the fundamental phase voltage, a common offset voltage, $E_{offset1}$ is added to the sinusoidal reference signals [5],[12], where the magnitude of $E_{offset1}$ is given by

$$E_{offset1} = -(E_{max} + E_{min})/2 \quad (12)$$

Where E_{max} and E_{min} are the maximum and minimum magnitudes of the three sampled sinusoidal reference signals respectively, in a sampling time interval. The addition of this common offset voltage, $E_{offset1}$, results in the active space vectors being centered in a sampling time interval, making the SPWM scheme equivalent to the SVPWM scheme [3]. In a sampling time interval, the sinusoidal reference signal which has lowest magnitude crosses the triangular carrier signal first, and causes the first transition in the inverter switching state. While the sinusoidal reference signal, which has the maximum magnitude, crosses the triangular carrier signal last and causes the last switching transition in the inverter switching states in a two-level SVPWM scheme [5],[13]. Thus the switching times of the active space vectors can be determined from the sampled sinusoidal reference signal amplitudes in a two-level inverter system [8].

The SPWM scheme, for seven-level inverter, sinusoidal reference signals are compared with symmetrical level shifted six triangular carrier signals for PWM generation [9]. After addition of offset voltage $E_{offset1}$ to the sinusoidal reference signals, the modified sinusoidal reference signals are shown in fig. 4 along with six triangular carrier signals. The sinusoidal reference signals cross the triangular carrier signals at different instants in a sampling time interval T_s (Fig. 4). Each time a sinusoidal reference signal crosses the triangular carrier signal, it causes a change in the inverter switching state. The changes in phase voltage and their time intervals are shown in Fig. 5 in a sampling time interval T_s . The sampling time interval T_s can be split into four time intervals t_{01} , t_1 , t_2 and t_{02} . The time intervals t_{01} and t_{02} are the time durations for the start and end inverter space vectors respectively, in a sampling time interval T_s . The time intervals t_1 and t_2 are the time durations for the middle inverter space vectors (active space vectors), in a sampling time interval T_s . It should be observed from Fig. 5 that the middle space vectors are not centered in a sampling time interval T_s . Because of the level-shifted six triangular carrier signals (Fig. 4), the first crossing (termed as *first_cross*) of the sinusoidal reference signal cannot always be the minimum magnitude of the three sampled sinusoidal reference signals, in a sampling time interval. Similarly, the last crossing (termed as *third_cross*) of the sinusoidal reference signal cannot always be the maximum magnitude of the three sampled sinusoidal reference signals, in a sampling time interval. Thus the offset voltage, $E_{offset1}$ is not sufficient to center the middle inverter space vectors, in a multilevel PWM system during a sampling time interval T_s (Fig. 5). Hence an additional offset (*offset2*) has to be added to the sinusoidal reference

signals of Fig. 4, so that the middle inverter space vectors can be centered in a sampling time interval, same as a two-level SVPWM system [3]. In this paper, a simple procedure to find out the offset voltage (to be added to the sinusoidal reference signals for PWM generation) is presented, based only on the sampled amplitudes of the sinusoidal reference signals. In the proposed scheme, the sinusoidal reference signal, from the three sampled sinusoidal reference signals, which crosses the triangular carrier signal first (*first_cross*) and the sinusoidal reference signal which crosses the triangular carrier signal last (*third_cross*) are found. Once the *first_cross* signal and *third_cross* signal are known, the theory of offset calculation of (12), for the 2-level inverter, can easily be adapted for the 7-level SVPWM generation scheme.

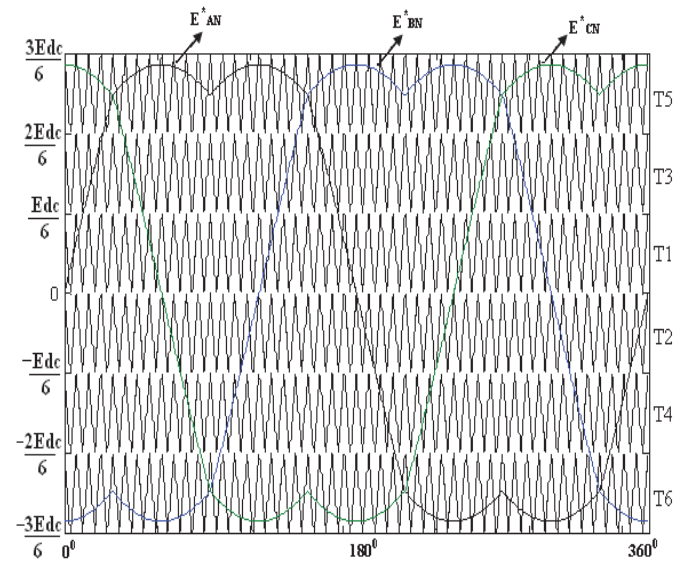


Fig. 4: Modified sinusoidal reference signals and triangular carrier signals for a seven-level PWM scheme

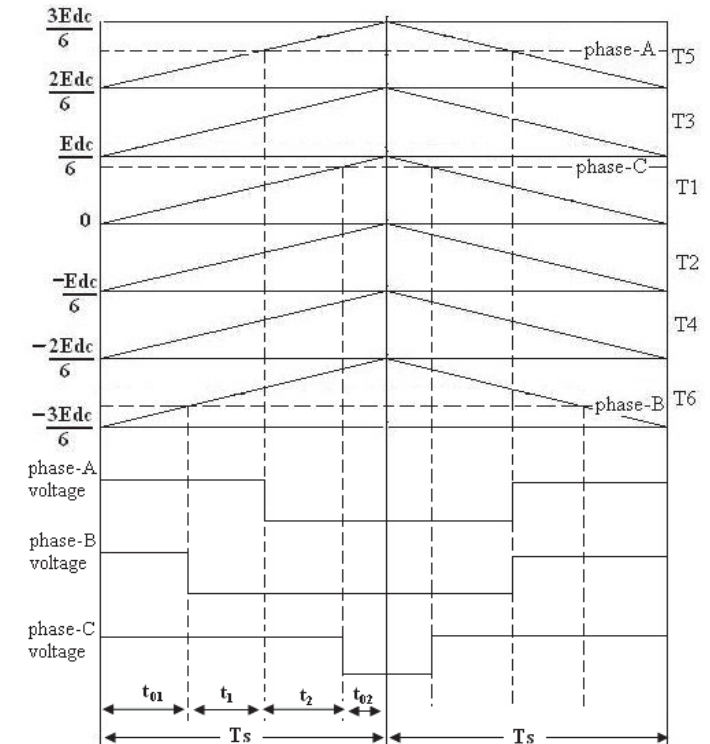


Fig. 5: Inverter switching vectors and their switching time durations during sampling time interval T_s

VI. DETERMINATION OF THE OFFSET VOLTAGE FOR A SEVEN-LEVEL INVERTER

Fig. 4 shows modified sinusoidal reference signals and six triangular Carrier signals used for PWM generation for seven-level inverter. The modified sinusoidal reference signals are given by

$$\begin{aligned} E_{AN}^* &= E_{AN} + E_{offset1} \\ E_{BN}^* &= E_{BN} + E_{offset1} \\ E_{CN}^* &= E_{CN} + E_{offset1} \end{aligned} \quad (13)$$

where E_{AN} , E_{BN} and E_{CN} are the sampled amplitudes of sinusoidal reference signals during the current sampling time interval and $E_{offset1}$ is calculated from (12). The time interval, at which the A-phase sinusoidal reference signal, E_{AN}^* crosses the triangular carrier signal, is termed as $T_{a-cross}$ (Fig. 6). Similarly, the time intervals, when the B-phase and C-phase sinusoidal reference signals, E_{BN}^* and E_{CN}^* cross the triangular carrier signals, are termed as $T_{b-cross}$ and $T_{c-cross}$ respectively. Fig. 6 shows a sampling time interval when the A-phase sinusoidal reference signal is in the triangular carrier region T5 while the B-phase sinusoidal reference signal and C-phase sinusoidal reference signal are in carrier region T6 and T1 respectively. As shown in Fig. 6, the time interval, $T_{a-cross}$, at which the A-phase sinusoidal reference signal crosses the triangular carrier signal is directly proportional to the phase voltage amplitude, $(E_{AN}^* - 2E_{dc}/6)$. The time interval, $T_{b-cross}$, at which the B-phase sinusoidal reference signal crosses the triangular carrier signal, is proportional to $(E_{BN}^* + 3E_{dc}/6)$ and the time interval, $T_{c-cross}$, at which the C-phase sinusoidal reference signal crosses the triangular carrier signal, is proportional to (E_{CN}^*) . Therefore

$$\begin{aligned} T_{a-cross} &= (E_{AN}^* - 2E_{dc}/6) \left(\frac{T_s}{E_{dc}/6} \right) = T^*_{as} - 2T_s \\ T_{b-cross} &= (E_{BN}^* + 3E_{dc}/6) \left(\frac{T_s}{E_{dc}/6} \right) = T^*_{bs} + 3T_s \\ T_{c-cross} &= (E_{CN}^*) \left(\frac{T_s}{E_{dc}/6} \right) = T^*_{cs} \end{aligned} \quad (14)$$

where T^*_{as} , T^*_{bs} and T^*_{cs} are the time equivalents of the voltage magnitudes. The proportionality between the time equivalents and corresponding voltage magnitudes is defined as follows [8]:

$$\begin{aligned} (E_{dc}/6)/T_s &= E_{AN}^*/T^*_{as} \\ (E_{dc}/6)/T_s &= E_{BN}^*/T^*_{bs} \\ (E_{dc}/6)/T_s &= E_{CN}^*/T^*_{cs} \\ (E_{dc}/6)/T_s &= E_{offset1}/T_{offset1} \end{aligned} \quad (15)$$

The time interval, at which the sinusoidal reference signals cross the triangular carrier signals for the first time, is termed as T_{first_cross} . Similarly, the time intervals, at which the sinusoidal reference signals cross the triangular carrier signals for the second and third time, are termed as, T_{second_cross} and T_{third_cross} respectively, in a sampling time interval T_s .

$$\begin{aligned} T_{first_cross} &= \min(T_{a-cross}, T_{b-cross}, T_{c-cross}) \\ T_{second_cross} &= \text{mid}(T_{a-cross}, T_{b-cross}, T_{c-cross}) \\ T_{third_cross} &= \max(T_{a-cross}, T_{b-cross}, T_{c-cross}) \end{aligned} \quad (16)$$

The time intervals, T_{first_cross} , T_{second_cross} and T_{third_cross} , directly decide the switching times for the different inverter voltage vectors, forming a triangular sector, during one sampling time interval T_s . The time intervals for the start and end space vectors, are $t_{01} = T_{first_cross}$, $t_{02} = (T_s - T_{third_cross})$, respectively (Fig. 5). The middle space vectors are centered by adding a time offset, $T_{offset2}$ to T_{first_cross} , T_{second_cross} and T_{third_cross} . The time offset, $T_{offset2}$ is determined as follows. The time interval for the middle inverter space vectors, T_{middle} , is given by:

$$T_{middle} = T_{third_cross} - T_{first_cross} \quad (17)$$

The time interval of the start and end space vector is

$$T_0 = T_s - T_{middle} \quad (18)$$

Thus the time interval of the start space vector is given by

$$T_0/2 = T_{first_cross} + T_{offset2}$$

Therefore

$$T_{offset2} = T_0/2 - T_{first_cross} \quad (19)$$

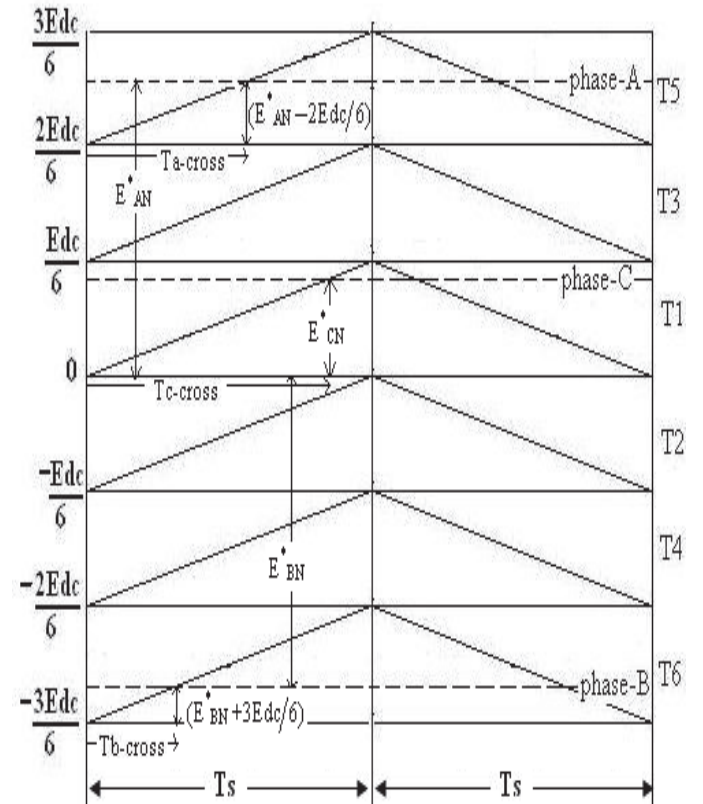


Fig. 6: Determination of the $T_{a-cross}$, $T_{b-cross}$ and $T_{c-cross}$ during sampling interval T_s

In this way, we can obtain offset voltages to be added for remaining samples during the time period of sinusoidal reference signal. For 7-level inverter maximum modulation index in the linear modulation range is 0.866 (the modulation index, M , is defined as the ratio of magnitude of the equivalent reference voltage space vector, generated by the three sinusoidal reference signals, to the DC link voltage). The proposed scheme can be adapted for modulation indices lesser than 0.866. The addition of the time offset, $T_{offset2}$ to $T_{a-cross}$, $T_{b-cross}$ and $T_{c-cross}$ gives the inverter leg switching times T_{ga} , T_{gb} and T_{gc} for phases A, B and C, respectively.

$$\begin{aligned}
Tga &= Ta - cross + Toffset2 \\
Tgb &= Tb - cross + Toffset2 \\
Tgc &= Tc - cross + Toffset2
\end{aligned}
\tag{20}$$

VII. SIMULATION RESULTS AND DISCUSSION

The proposed SVPWM scheme is simulated using MATLAB environment with open loop E/f control for different modulation indices. The respective DC link voltages are $(2/6)E_{dc}$, $(2/6)E_{dc}$, $(1/6)E_{dc}$ and $(1/6)E_{dc}$ for the INV-1, INV-2, INV-3 and INV-4, where E_{dc} is the DC link voltage of an equivalent conventional single two-level inverter drive. The speed reference is translated to the frequency and voltage commands maintaining E/f. The modified three reference sinusoidal signals which are added by the total offset voltage to make SPWM scheme equivalent to the SVPWM scheme, are simultaneously compared with the triangular carrier set. A DC link voltage (E_{dc}) of 600 volts is assumed for simulation studies. Fig. 7a shows the motor phase voltage (E_{A2A4}) in the lowest speed range which corresponds to layer-1 operation (two-level mode) when modulation index is 0.13. Fig. 7b shows the total offset voltage to be added to sinusoidal reference signals to make SPWM equivalent to the SVPWM and fig. 7c shows the A-phase sinusoidal reference signal after offset voltage is added. During this range of operation, motor phase current and normalized harmonic spectrum of motor phase voltage are shown in Fig. 7d and Fig. 7e respectively. Fig. 8a shows the motor phase voltage (E_{A2A4}) in the next speed range which corresponds to layer-2 operation (three-level mode) when modulation index is 0.25. Fig. 8b shows the total offset voltage to be added to sinusoidal reference signals to make SPWM equivalent to the SVPWM and fig. 8c shows the A-phase sinusoidal reference signal after offset voltage is added. During this range of operation, motor phase current and normalized harmonic spectrum of motor phase voltage are shown in Fig. 8d and Fig. 8e respectively. Fig. 9a shows the motor phase voltage (E_{A2A4}) in the next speed range which corresponds to layer-3 operation (four-level mode) when modulation index is 0.425. Fig. 9b shows the total offset voltage to be added to sinusoidal reference signals to make SPWM equivalent to the SVPWM and fig. 9c shows the A-phase sinusoidal reference signal after offset voltage is added. During this range of operation, motor phase current and normalized harmonic spectrum of motor phase voltage are shown in Fig. 9d and Fig. 9e respectively. Fig. 10a shows the motor phase voltage (E_{A2A4}) in the next speed range which corresponds to layer-4 operation (five-level mode) when modulation index is 0.55. Fig. 10b shows the total offset voltage to be added to sinusoidal reference signals to make SPWM equivalent to the SVPWM and fig. 10c shows the A-phase sinusoidal reference signal after offset voltage is added. During this range of operation, motor phase current and normalized harmonic spectrum of motor phase voltage are shown in Fig. 10d and Fig. 10e respectively. Fig. 11a shows the motor phase voltage (E_{A2A4}) in the next speed range which corresponds to layer-5 operation (six-level mode) when modulation index is 0.7. Fig. 11b shows the total offset voltage to be added to sinusoidal reference signals to make SPWM equivalent to the SVPWM and fig. 11c shows the A-phase sinusoidal reference signal after

offset voltage is added. During this range of operation, motor phase current and normalized harmonic spectrum of motor phase voltage are shown in Fig. 11d and Fig. 11e respectively. Fig. 12a shows the motor phase voltage (E_{A2A4}) in the next speed range which corresponds to layer-6 operation (seven-level mode) when modulation index is 0.85. Fig. 12b shows the total offset voltage to be added to sinusoidal reference signals to make SPWM equivalent to the SVPWM and fig. 12c shows the A-phase sinusoidal reference signal after offset voltage is added. During this range of operation, motor phase current and normalized harmonic spectrum of motor phase voltage are shown in Fig. 12d and Fig. 12e respectively. The ratio of triangular carrier signal frequency to reference sinusoidal signal frequency is 48 for all ranges of operation. It can be observed that the motor phase voltage and motor phase current during 7-level operation are very smooth and close to the sinusoid with lower harmonics.

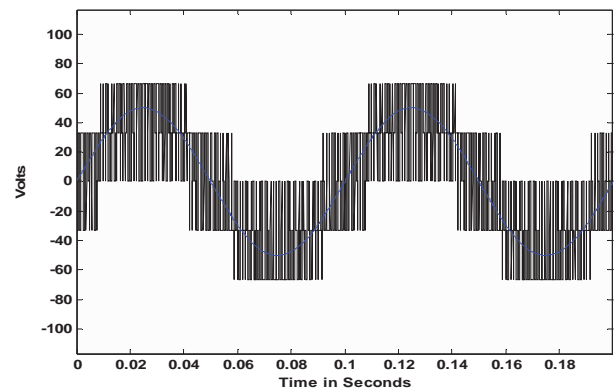


Fig. 7a: Motor phase voltage when $M=0.13$ (layer-1, 2-level operation)

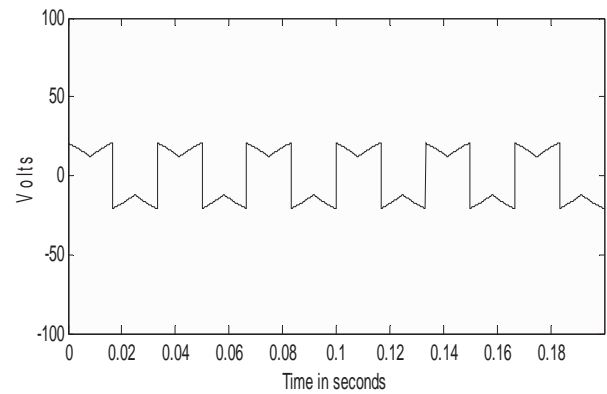


Fig. 7b: The offset voltage to be added to sinusoidal reference signals when $M=0.13$ (layer-1, 2-level operation)

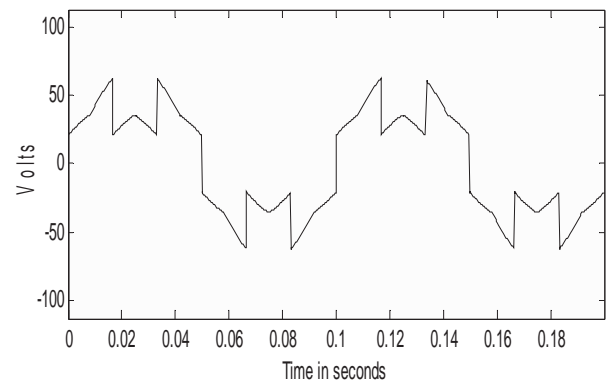


Fig. 7c: The A-phase sinusoidal reference signal after offset voltage is added when $M=0.13$ (layer-1, 2-level operation)

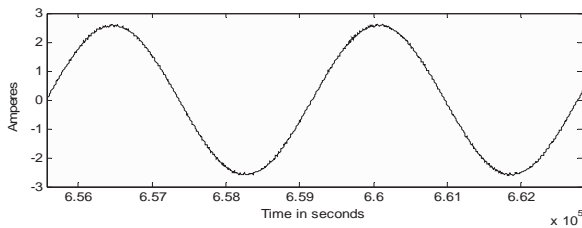


Fig. 7d: Motor phase current when $M=0.13$ (layer-1, 2-level operation)

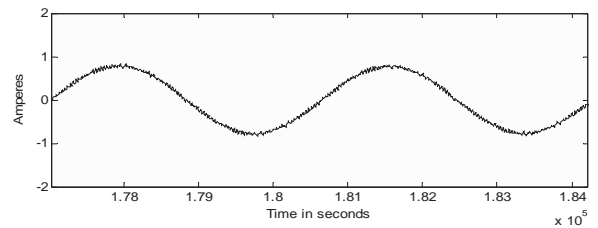


Fig. 8d: Motor phase current when $M=0.25$ (layer-2, 3-level operation)

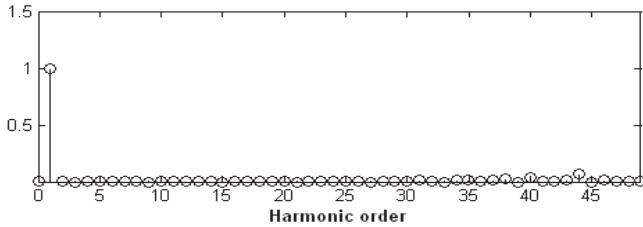


Fig. 7e: Normalized harmonic spectrum of the motor phase voltage when $M=0.13$ (layer-1, 2-level operation)

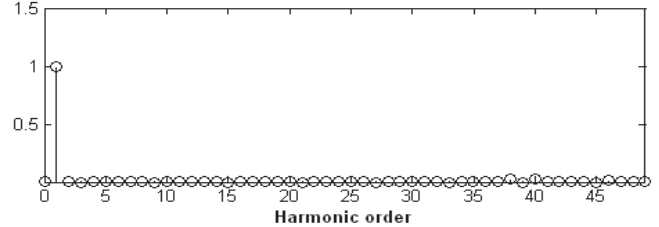


Fig. 8e: Normalized harmonic spectrum of the motor phase voltage when $M=0.25$ (layer-2, 3-level operation)

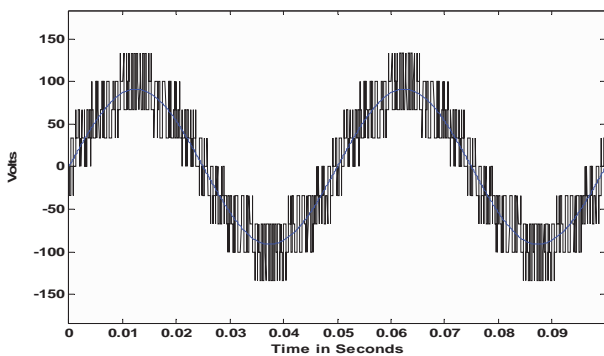


Fig. 8a: Motor phase voltage when $M=0.25$ (layer-2, 3-level operation)

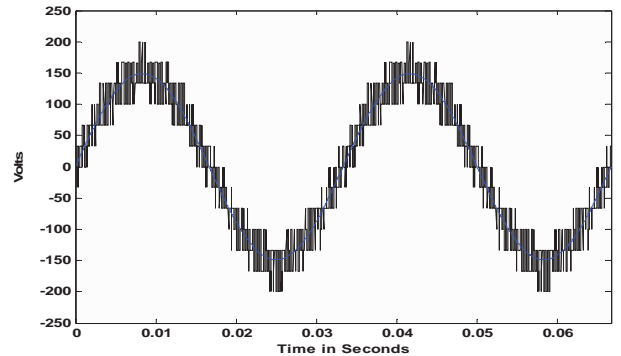


Fig. 9a: Motor phase voltage when $M=0.425$ (layer-3, 4-level operation)

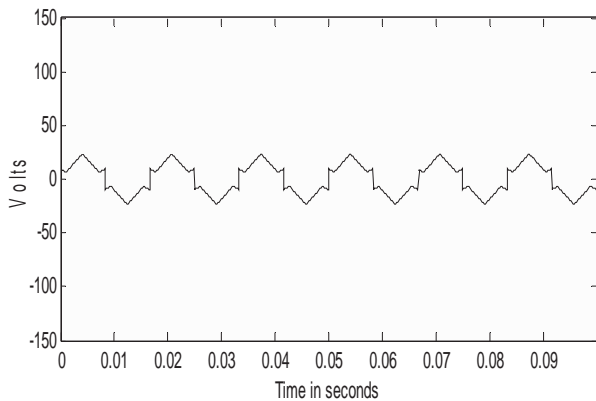


Fig. 8b: The offset voltage to be added to sinusoidal reference signals when $M=0.25$ (layer-2, 3-level operation)

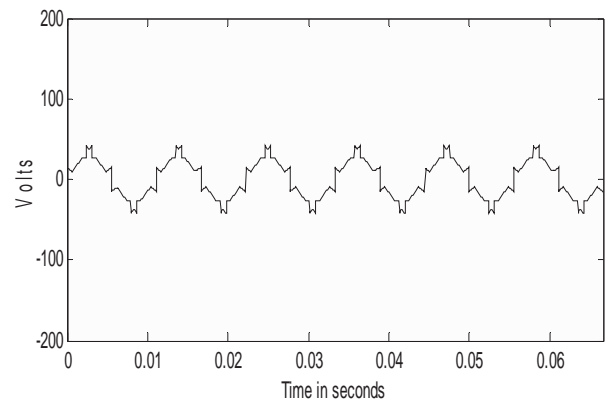


Fig. 9b: The offset voltage to be added to sinusoidal reference signals when $M=0.425$ (layer-3, 4-level operation)

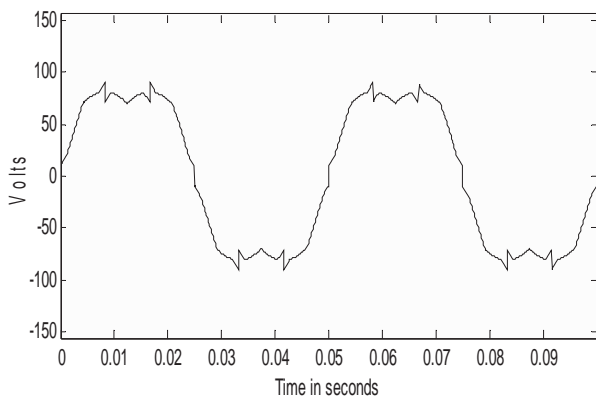


Fig. 8c: The A-phase sinusoidal reference signal after offset voltage is added when $M=0.25$ (layer-2, 3-level operation)

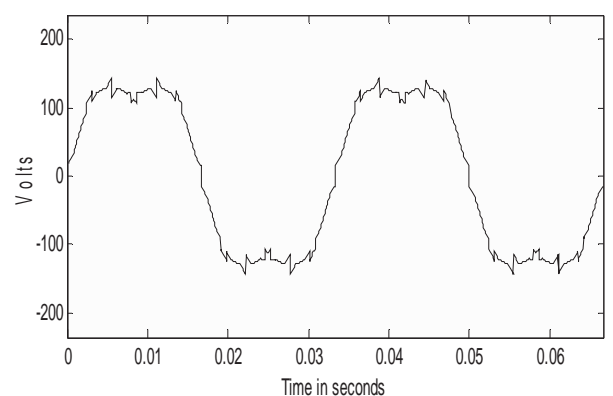


Fig. 9c: The A-phase sinusoidal reference signal after offset voltage is added when $M=0.425$ (layer-3, 4-level operation)

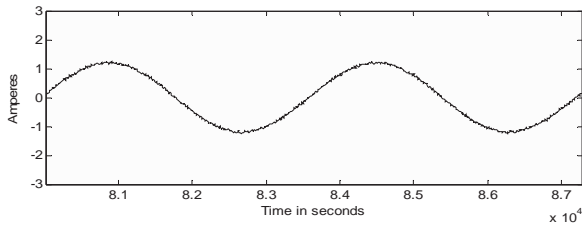


Fig. 9d: Motor phase current when $M=0.425$ (layer-3, 4-level operation)

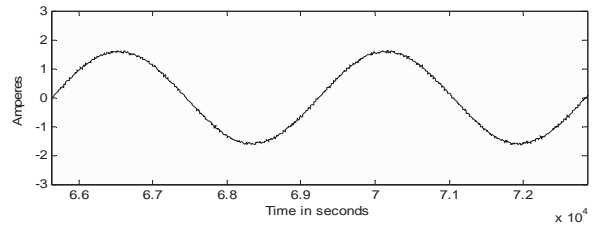


Fig. 10d: Motor phase current when $M=0.55$ (layer-4, 5-level operation)

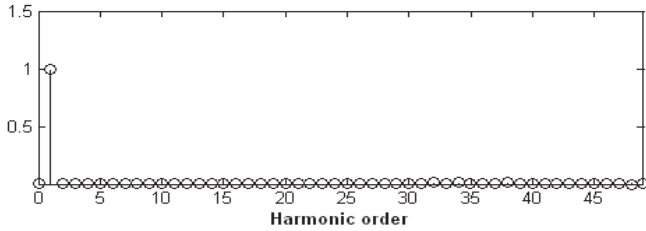


Fig. 9e: Normalized harmonic spectrum of the motor phase voltage when $M=0.425$ (layer-3, 4-level operation)

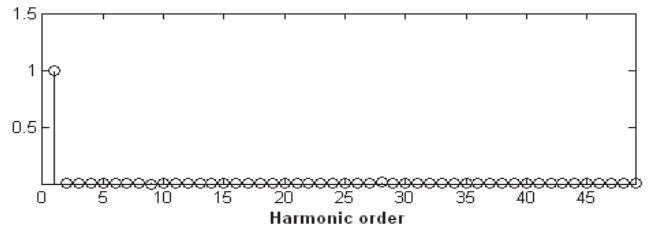


Fig. 10e: Normalized harmonic spectrum of the motor phase voltage when $M=0.55$ (layer-4, 5-level operation)

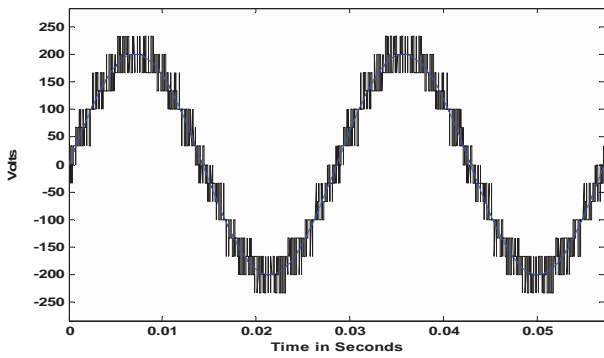


Fig. 10a: Motor phase voltage when $M=0.55$ (layer-4, 5-level operation)

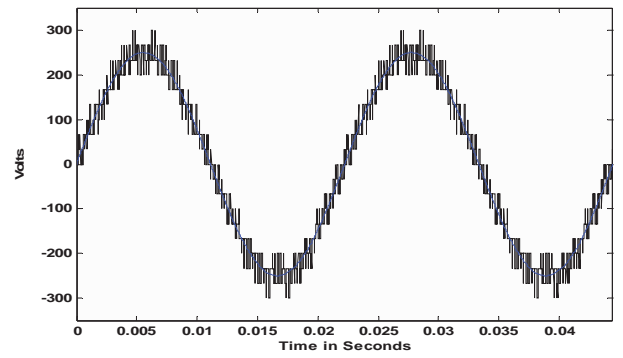


Fig. 11a: Motor phase voltage when $M=0.7$ (layer-5, 6-level operation)

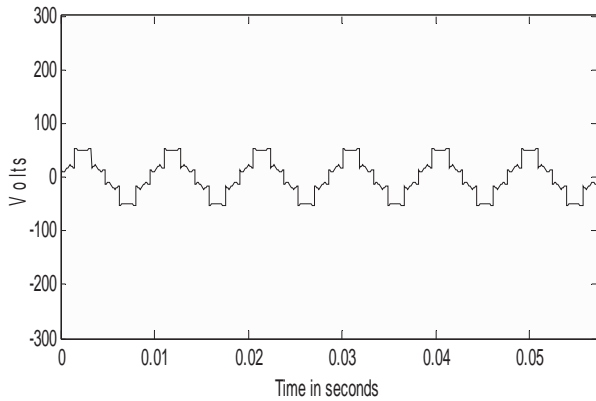


Fig. 10b: The offset voltage to be added to sinusoidal reference signals when $M=0.55$ (layer-4, 5-level operation)

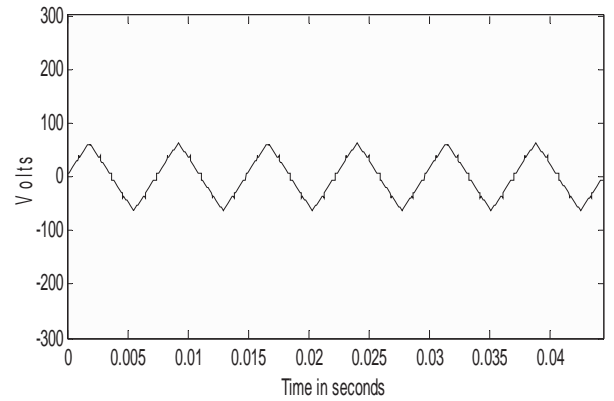


Fig. 11b: The offset voltage to be added to sinusoidal reference signals when $M=0.7$ (layer-5, 6-level operation)

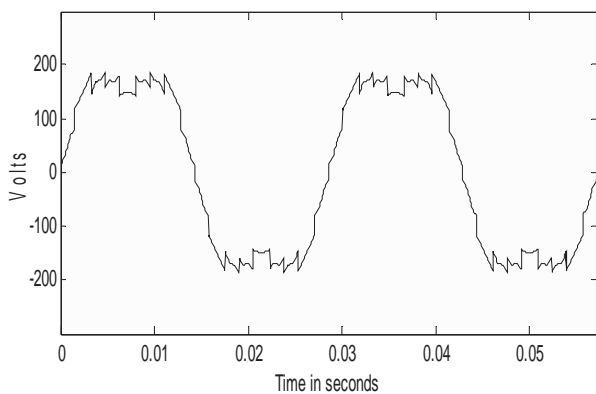


Fig. 10c: The A-phase sinusoidal reference signal after offset voltage is added when $M=0.55$ (layer-4, 5-level operation)

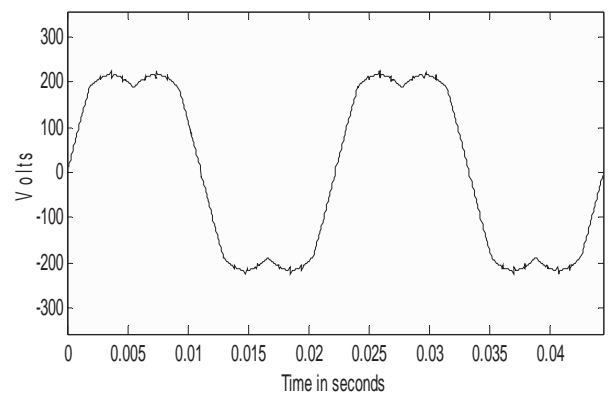


Fig. 11c: The A-phase sinusoidal reference signal after offset voltage is added when $M=0.7$ (layer-5, 6-level operation)

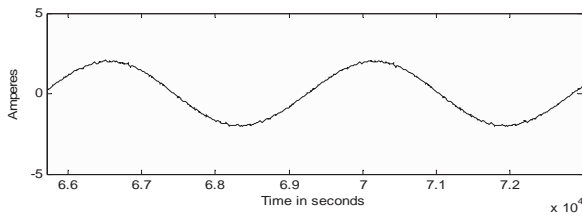


Fig. 11d: Motor phase current when $M=0.7$ (layer-5, 6-level operation)

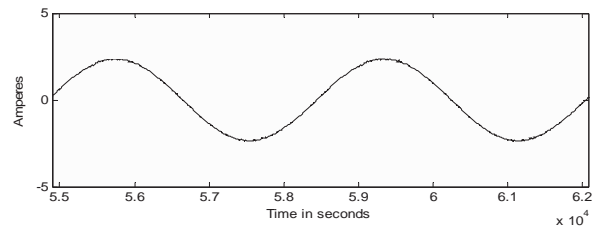


Fig. 12d: Motor phase current when $M=0.85$ (layer-6, 7-level operation)

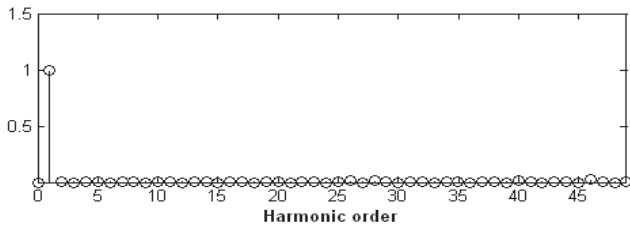


Fig. 11e: Normalized harmonic spectrum of the motor phase voltage when $M=0.7$ (layer-5, 6-level operation)

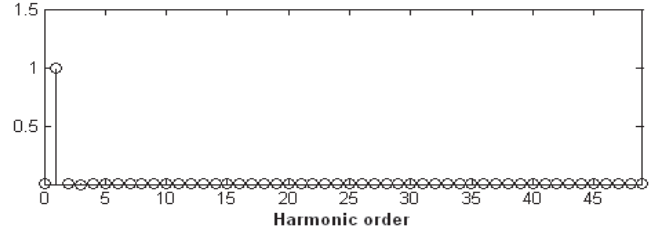


Fig. 12e: Normalized harmonic spectrum of the motor phase voltage when $M=0.85$ (layer-6, 7-level operation)

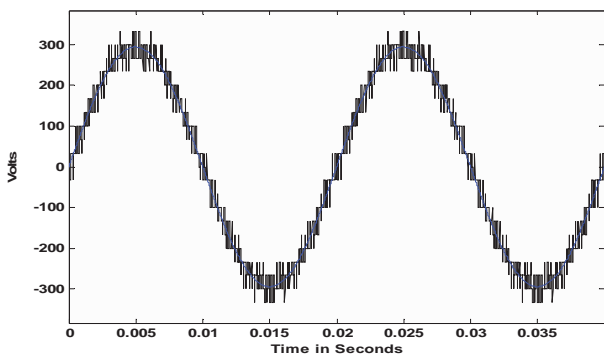


Fig. 12a: Motor phase voltage when $M=0.85$ (layer-6, 7-level operation)

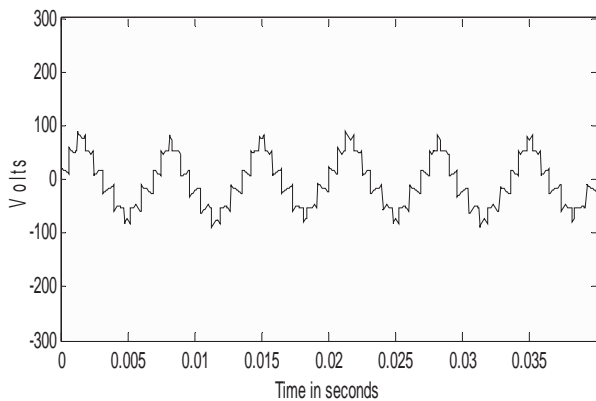


Fig. 12b: The offset voltage to be added to sinusoidal reference signals when $M=0.85$ (layer-6, 7-level operation)

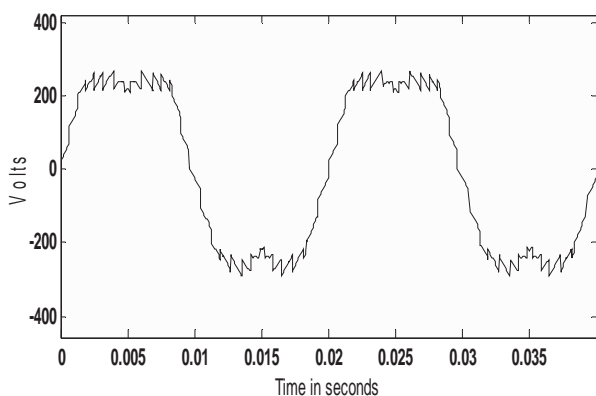


Fig. 12c: The A-phase sinusoidal reference signal after offset voltage is added when $M=0.85$ (layer-6, 7-level operation)

VIII. CONCLUSION

A modulation scheme of SVPWM for seven-level inverter system for dual-fed induction motor drive, where the induction motor is fed by two symmetrical three-level inverters from both ends is presented. The symmetrical three-level inverter used is composed of two conventional two-level inverters with equal DC link voltage in cascade. The centering of the middle inverter space vectors of the SVPWM is accomplished by the addition of an offset voltage signal to the sinusoidal reference signals, derived from the sampled amplitudes of the sinusoidal reference signals. The SVPWM technique, presented in this paper does not require any sector identification, as is required in conventional SVPWM schemes. The proposed scheme eliminates the use of look-up table approach to switch the appropriate space vector combination as in conventional SVPWM schemes. This reduces the computation time required to determine the switching times for inverter legs, making the algorithm suitable for real-time implementation.

REFERENCES

- [1] Holtz, J., "Pulsewidth modulation—A survey", *IEEE Trans. Ind. Electron.*, vol. 30, no.5, pp. 410–420, 1992.
- [2] Zhou, K., and Wang, D., "Relationship between space-vector modulation and three-phase carrier-based PWM: A comprehensive analysis", *IEEE Trans. Ind. Electron.*, vol. 49, no.1, pp. 186–196, 2002.
- [3] Van der Broeck, Skudelny, H.C., and Stanke, G.V., "Analysis and realisation of a pulsewidth modulator based on voltage space vectors", *IEEE Trans. Ind. Appl.*, vol. 24, no. 1, pp. 142–150, 1988.
- [4] Boys, J.T., and Handley, P.G., "Harmonic analysis of space vector modulated PWM waveforms", *IEE Proc. Electr. Power Appl.*, vol. 137, no. 4, pp. 197–204, 1990.
- [5] Holmes, D.G., "The general relationship between regular sampled pulse width modulation and space vector modulation for hard switched converters", *Conf. Rec. IEEE Industry Applications Society (IAS) Annual Meeting*, pp. 1002–1009, 1992.
- [6] Holtz, J., Lotzkat, W., and Khambadkone, A., "On continuous control of PWM inverters in over-modulation range including six-step mode", *IEEE Trans. Power Electron.*, vol. 8, no. 4, pp. 546–553, 1993.
- [7] Lee, D., and Lee, G., "A novel overmodulation technique for

- space vector PWM inverters”, *IEEE Trans. Power Electron.*, vol. 13, no. 6, pp. 1144–1151, 1998.
- [8] Kim, J., and Sul, S., “A novel voltage modulation technique of the Space Vector PWM”, *Proc. Int. Power Electronics Conf.*, Yokohama, Japan, pp. 742–747, 1995.
- [9] Carrara, G., Gardella, S.G., Archesoni, M., Salutari, R., and Sciotto, G., “A new multi-level PWM method: A theoretical analysis”, *IEEE Trans. Power Electron.*, vol. 7, no. 3, pp. 497–505, 1992.
- [10] Shivakumar, E.G., Gopakumar, K., Sinha, S.K., Andre, Pittet, and Ranganathan, V.T., “Space vector PWM control of dual inverter fed open-end winding induction motor drive”, *Proc. Applied Power Electronics Conf. (APEC)*, pp. 339–405, 2001.
- [11] Suh, J., Choi, C., and Hyun, D., “A new simplified space vector PWM method for three-level inverter”, *Proc. IEEE Applied Power Electronics Conf. (APEC)*, pp. 515–520, 1999.
- [12] Baiju, M.R., Mohapatra, K.K., Somasekhar, V.T., Gopakumar, K., and Umanand, L., “A five-level inverter voltage space phasor generation for an open-end winding induction motor drive”, *IEE Proc. Electr. Power Appl.*, vol. no. 5, pp. 531–538, 2003.
- [13] Wang, FEL., “Sine-triangle versus space vector modulation for threelevel PWM voltage source inverters”, *Proc. IEEE-IAS Annual Meeting*, Rome, pp. 2482–2488, 2000.
- [14] Baiju, M.R., Gopakumar, K., Somasekhar, V.T., Mohapatra, K.K., and Umanand, L., “A space vector based PWM method using only the instantaneous amplitudes of reference phase voltages for three-level inverters”, *EPE J.*, vol. 13, no. 2, pp. 35–45, 2003.
- [15] McGrath, B.P., Holmes, D.G., and Lipo, T.A., “Optimized space vector switching sequences for multilevel inverters”, *Proc. IEEE Applied Power Electronics Conf. (APEC)*, pp. 1123–1129, 2001.
- [16] Krah, J., and Holtz, J., “High performance current regulation and efficient PWM Implementation for low inductance servo motors”, *IEEE Trans. Ind. Appl.*, vol. 36, no. 5, pp. 1039–1049, 1999.
- [17] Somasekhar, V.T., and Gopakumar, K., “Three-level inverter configuration cascading two 2-level inverters”, *IEE Proc. Electr. Power Appl.*, vol. 150, no. 3, pp. 245–254, 2003.
- [18] R.S.Kanchan, M.R.Baiju, K.K.Mohapatra, P.P.Ouseph and K.Gopakumar., “Space vector PWM signal generation for multilevel inverters using only the sampled amplitudes of reference phase voltages”, *IEE Proc.-Electr. Power Appl.*, vol. 152, no. 2, pp.297-309, March 2005.
- [19] M.R.Baiju, K.Gopakumar, K.K.Mohapatra, V.T Somasekhar and L.Umanand, “Five-Level inverter voltage-space vector phasor generation for an Open-End Winding Induction Motor Drive”. *IEE proc.-power Appl.*, vol. 150, no. 5, pp.531-538, Sep. 2003.
- [20] G.Sambasiva Rao and K.Chandra Sekhar “seven-Level Inverter System for Dual-Fed Induction Motor Drive”, *International journal of Electrical engineering and technology*. vol.1, no.1, pp.9-22, 2011.

BIOGRAPHIES



G. Sambasiva Rao received B.E. degree in Electrical and Electronics Engineering from Andhra University Engineering College, Visakha Patnam, India in 2000 and M.E. with Power Electronics and Industrial Drives from Sathyabama Institute of Science and Technology, Chennai, India in 2006. Since 2006, he has been with R.V.R and J.C.College of engineering as Lecturer. Presently he is a part-time research student at J.N.T.U College of Engineering, Hyderabad- 500072, India, working towards his doctoral degree.



K. Chandra Sekhar received his B.Tech degree in Electrical and Electronics Engineering from V.R.Siddartha Engineering College, Vijayawada, India in 1991 and M.Tech with Electrical Machines and Industrial Drives from Regional Engineering College, Warangal, India in 1994. He Received the PhD degree from the J.N.T.U College of Engineering, Hyderabad- 500072, India in 2008. He is having 16 years of teaching experience. He is currently Head of Department, EEE, R.V.R and J.C.College of engineering, Guntur, India. His Research interests are Power Electronics, Industrial Drives & FACTS Devices.